# ZrN coatings deposited by high power impulse magnetron sputtering and cathodic arc techniques.

PURANDARE, Yashodhan, EHIASARIAN, Arutiun, SANTANA, Antonio and HOVSEPIAN, Papken



**Published version**

PURANDARE, Yashodhan, EHIASARIAN, Arutiun, SANTANA, Antonio and HOVSEPIAN, Papken (2014). ZrN coatings deposited by high power impulse magnetron sputtering and cathodic arc techniques. Journal of Vacuum Science & Technology A, 32 (3).

# ZrN coatings deposited by High Power Impulse Magnetron Sputtering and Cathodic Arc Techniques.

**Running title:** ZrN coatings by HIPIMS and CA.

**Running authors:** Purandare et.al.

Y. P. Purandare[a)1)], A. P. Ehiasarian[a)], A. Santana[b)], and P. Eh Hovsepian[a)]

[a)] *Nanotechnology Centre for PVD Research, Materials and Engineering Research Institute, Sheffield Hallam University, UK S1 1WB.*

[b)] *Ionbond AG Olten, Industriestrasse 211, CH-4600 Olten.*

[1)]Corresponding author: Phone: +44-114-225 3469, Fax: +44-114-225-3501.

[1)]Email: Y.Purandare@shu.ac.uk.

Zirconium nitride (ZrN) coatings were deposited on 1 micron finish High Speed Steel (HSS) and 316L Stainless Steel (SS) test coupons. Cathodic Arc (CA) and HIPIMS (High Power Impulse Magnetron Sputtering) + UBM (Unbalanced Magnetron Sputtering) techniques were utilised to deposit coatings. CA plasmas are known to be rich in metal and gas ions of the depositing species as well as macro-particles (droplets) emitted from the arc sports. Combining HIPIMS technique with UBM in the same deposition process facilitated increased ion bombardment on the depositing species during coating growth maintaining high deposition rate. Prior to coating deposition, substrates were pretreated with $Zr^+$ rich plasma, for both arc deposited and HIPIMS deposited coatings, which led to a very high scratch adhesion value ($L_{C2}$) of 100 N. Characterisation results revealed the overall thickness of the coatings in the range of 2.5 µm with hardness in the range of 30-40 GPa depending on the deposition technique. Cross-sectional Transmission Electron Microscopy (TEM), tribological experiments such as dry sliding wear tests and corrosion studies have been utilised to study the effects of ion bombardment on the structure and properties of these coatings. In all the cases HIPIMS assisted UBM deposited coating fared equal or better than the arc deposited coatings, the reasons being discussed in this paper. Thus H+U coatings provide a good alternative to arc deposited where smooth, dense coatings are required and macro droplets cannot be tolerated.

# I. Introduction

Zirconium nitride (ZrN) coatings due to its inherent high hardness, wear resistance, corrosion resistance and gold like colour have attracted many applications ranging from coatings for wear resistance, corrosion resistance, coatings for bio-medical appliances, high reflectivity optical and decorative surfaces. PVD coating properties have shown a strong relationship with their density[1,2] demonstrating superior properties with increasing compactness. In the case of reactively sputtered films, often higher bias voltages, temperatures[3] or auxiliary ionisation devices have been utilised to reduce growth related (shadowing) defects[4]. Microstructure of arc evaporated coatings is free of inter columnar voids however the areas surrounding a droplet is defective and can lead to under- dense structures.[5,6] Magnetron sputtered coatings are free from droplets however are known to be under-dense due to the lower mobility of the condensing species available during the growth[7]. ZrN has been successfully deposited with arc evaporation[8], reactive sputtering[9] and by Plasma Based Ion Implantation and Deposition (PBII&D) process where high negative pulses were employed to control ion energy bombardment during film growth.[10] Though arc technique remains a popular choice due to its high deposition rate, the possibility of depositing dense and defect free ZrN has to be exploited.

High Power Impulse Magnetron Sputtering (HIPIMS) serves as a new deposition technology addressing problems of arc and magnetron sputtering deposition. HIPIMS generates highly ionised plasmas, rich with metal and working gas ions[2,11] which can be effectively used for surface pre-treatment.[2] Intense low energy ion bombardment (ionised deposition flux) of the growing films during deposition with this technique results in dense structures and smoother surface finish.[2] A general overview of HIPIMS technique can be found in the review article.[12] Similarly the Cathodic Arc (CA) process is very rich in metal and gas ions with multiple charge states and high energies, resulting in intense metal ion bombardment during deposition.[13]

Arc deposition has been thoroughly studied for most nitrides. Because of the intense high energy ion bombardment during deposition the droplet free volumes of the films can be very dense similar to the structure of the coatings deposited by the novel HIPIMS technique. With this view the current study focuses on the comparison between ZrN coatings deposited by the Cathodic Arc (CA) and HIPIMS + Unbalanced Magnetron Sputtering (UBM) technology

(denoted as H+U hereafter). UBM has been retained in the process to achieve higher deposition rates than achieved in pure HIPIMS processes.

## II. Experiments

### A. Coating deposition

The ZrN coatings were deposited on High Speed Steel (HSS) and 304S Stainless Steel (SS) substrates polished to 1 micron finish. Prior to the coating deposition, Zr metal ion etching (Zr+) was utilised for the pretreatment of the substrates. For the CA coatings steered CA technique was employed to clean the substrates where the substrates were biased at -900 V. For the H+U process Zr ions generated with the help of HIPIMS plasma were utilised and the substrates were biased at -600 V.

DC CA ZrN coatings were deposited in an IB RoadRunner machine (target to substrate distance of 155 mm) with 70A cathode current and substrate bias voltage ($U_b$) of -65V in the temperature range of 200°C. H+U coatings were deposited in an industrial size machine (HTC 1000- 4 target system (Hauzer Techno Coatings, Europe B.V., Venlo, The Netherlands) enabled with HIPIMS power supplies (Hüttinger Electronic Sp. z o.o., Warsaw, Poland) at Sheffield Hallam University. For coating deposition, 2 zirconium targets, namely one in HIPIMS mode and one in UBM mode were used (target to substrate distance of 155 mm). Rectangular pulses of 200 µs, with a peak current of 200 A and duty cycle of 1% were employed to generate the HIPIMs plasma for coating deposition. Based on the results from a previous work, Purandare et. al,[14] a substrate bias voltage ($U_b$) of -75 V was chosen whereas the deposition temperature of 400° C was employed to provide a cleaner deposition environment. The details of the machine and cathode arrangement can be found in the previous publication.[14]

### B. Coating characterisation

These coating were extensively characterised by various analytical techniques:

1. The texture and the residual stress in the coating were determined by Bragg-Brentano (2θ, 20-130°) geometry in a PHILIPS XPERT XRD machine. The crystallite sizes within the columnar grains were calculated by the Scherrer equation by measuring the peak broadening at half the maximum intensity (FWHM).

2. Hardness and Young's modulus (E) was measured with a CSM nanoindenter with a maximum load of 20 mN. The Oliver and Pharr technique (O&P) was used to calculate these values.

3. Coating adhesion (critical load ($L_{C2}$) of coating failure) was measured with CSEM REVETEST under progressive loading conditions. The normal load was progressively increased from 5N to 100N at the rate of 0.01$Nm^{-1}$ (10N/mm) with an indenter moving at a velocity of 1.6 x $10^{-4}$ $ms^{-1}$ (10mm/min).

4. Tribological properties of the coating were examined by subjecting the coated HSS specimens to dry sliding wear experiments at ambient temperatures. Dry sliding wear coefficients ($K_C$) and friction coefficient were measured with a pin on disk apparatus (CSM TRIBOMETER). The counterpart consisted of a 6 mm $Al_2O_3$ ball and a constant load of 5 N was applied on the specimens which were sliding at a linear speed of 0.1 $ms^{-1}$ for 3760 m (60,000 laps). Dektak-150 stylus profiler was used to measure the wear tracks and topographical features of the coating.

5. Coating microstructure cross-sections were observed using with cross-sectional Transmission Electron Microscopy (Phillips EM 420 and CM20) and Scanning Electron Microscopy (FEI NOVA-NANOSEM 200, SIRION XL30) studies. Topographical features of the coating surface were also obtained by using a CSM Atomic force Microscope (AFM).

6. Spectrophotometery: A MINOLTA (CM-508d) Spectrophotometer with an incident angle of 10° and a D 65 illuminant was used to measure the colour of the ZrN coatings. The experiments were performed to quantify the colour in the form of L*a*b* colour system.

7. Corrosion: Princeton 263A corrosion monitoring apparatus was used to polarise the specimens in a 3.5% NaCl solution from -1000 mV to +1000 mV. The sweep rate of 0.5 $mVs^{-1}$ was utilised.

# III. Results and discussions

## A. Characterisation results

Coatings were extensively characterised for their mechanical, tribological properties and microstructure analysis. The characterisation results are presented in table 1.

The thickness of the coatings was investigated with a ball cratering method and was found to be 2.5± 0.2 microns for both the techniques. For the current set of deposition conditions, the H+U process had a deposition rate of 0.62 $\mu mhr^{-1}$ whereas the CA process the deposition rate was calculated to be 0.85 $\mu mhr^{-1}$. Results from the scratch adhesion testing demonstrated that irrespective of the deposition technology, the coatings exhibited strong adhesion to the substrate.

No adhesive failure (spallation) was observed until the applied progressive load reached 100 N at which through coating penetration was apparent. Both deposition techniques had involved substrate cleaning pre-treatment, wherein the surface was bombarded with $Zr^+$ ions. This intense bombardment with metal ions during the pre-treatment achieved by HIPIMS,[11] in this case $Zr^+$ ions, leads to the effective cleaning of the surface and to the implantation of Zr ions resulting in epitaxial growth of the coating.[14,15] Thus pre-treatment with HIPIMS leads to good adhesion of magnetron sputtered coatings, comparable to those achieved with CA processes, however with the benefits of avoiding droplet deposition.

Figure 1 shows the X-ray diffractograms obtained for the ZrN deposited on stainless steel substrates. As evident from the results, the coating has a FCC-NaCl structure. Coatings deposited with H+U technique show a mixed texture however with a dominating (111) and (200) directions. It has been reported that ZrN coatings deposited by MS technique show an increase in (111) and (200) peaks with higher negative bias voltages (a result of high ion bombardment with increasing bias).[2,16] Similarly in the previous work for ZrN deposition exclusively by HIPIMS,[13] a rise in (111) orientation was observed with increasing bias voltage. Thus in the current set of results higher ion bombardment (metal and reactive gas ions) originating from HIPIMS plasma (therefore higher ad-atom mobility) can be attributed for the rise of (111) peak in the H+U coatings. Literature for ZrN by arc technique report (200) being the dominant texture where the authors suggest that an increase in the deposition

temperature can lead to an increment in (111) contributions.[17,18] Thus for the current set of CA coatings lower bias voltage, as well as a different plasma chemistry (different metal to gas ion ratios as well as reactive to process gas ion ratio) can be attributed for a strong (200) peak.

The effect of ion bombardment on the crystallite sizes (present within the columnar grains) is evident from table no 2. The two prominent peaks observed in this study, namely (111) and (200) were used to calculate the crystallite sizes and lattice strains by the Scherrer equation. H+U coating shows lower crystallite sizes and higher strain values whereas CA coating shows higher crystallite sizes and lower strain values for all reflections. Consequently CA coatings show a higher compressive stress value of -5.82 ± 0.3 GPa whereas H+U coating showed a compressive stress value of - 4.12 ± 0.2 GPa.

Loading and unloading curves obtained from the nanoindentation results revealed a high hardness of 35 ± 3 GPa for the H+U coating which was comparable to those of CA coatings with a hardness of 37 ± 3.4 GPa. Despite having the same hardness, H+U coating fared better in dry sliding conditions ($K_C = 5.3 \times 10^{-15}$ $m^3N^{-1}m^{-1}$) than the CA coatings ($K_C = 8.01 \times 10^{-15}$ $m^3N^{-1}m^{-1}$). The high hardness and better wear resistance of the H+U coating can be attributed to the dense, defect free micro structure (free from droplet and under dense structures which form weak points in the coating).[19]

## B. Microstructure analysis

The microstructure of PVD coatings depend on a number of factors such as deposition pressure, temperature and available ion bombardment. All these parameters in turn affect the ad-atom mobility of the condensing species. HIPIMS is well known to have high metal ion content which can be tailored to either clean the surface as in pre-treatment or deposit dense structures. In a previous publication from the authors, it was demonstrated that pure HIPIMS technique and consequently the intense low energy ion bombardment from the depositing species can be used to deposit very dense ZrN coatings.[14] These coatings were shown to have a very dense and highly textured microstructure with wide and flat columns, and difficult to resolve grain boundaries. In the current set of experiments UBM technique was combined with HIPIMS to compensate for the drop in the deposition rate by HIPIMS.

Figure 2 shows a bright-field TEM image of the H+U coating cross-section along with the selected area diffraction patterns in the inset. As observed in the micrograph, a dense coating (with no inter-columnar voids) with a sharp and flat interface between the substrate and the coating can be clearly seen. Just above the substrate-coating interface, a band of coating growth, extended throughout cross-section width, is seen with the same contrast as that of the substrate. As evident from the diffraction pattern, this band is a result of the epitaxial growth which is a finger print of HIPIMS etching.[11] This epitaxial growth, at many places in the cross-section, is seen extended towards the top of the coating. The columnar grains (widths in the range of 200 -300 nm) are very densely packed to the extent that columnar grain boundaries are difficult to resolve[19] and the coating is without any droplet inclusions. The coating retains dome-shaped column tops as also seen from the AFM image (figure 4a), a signature feature of magnetron sputtered coatings,[19] however much flatter and without the usual inter-columnar voids (as compared to UBM coatings only). This microstructure is a result of the ionised depositing flux achieved by combining HIPIMS with UBM.

Figure 3 shows the cross-sectional view of the CA coating captured in the bright-field mode of the TEM. Microstructure of arc coatings can lack large area epitaxy which was also evident from the contrast and the selected area diffracted pattern for the current set of coatings (figure 3). Though the interface appears flat in the current micro-graph, it can be disturbed by the depositing droplets often associated in steered Cathodic Arc pre-treatment and in the deposition steps. The columnar microstructure of CA coating appears dense (widths also in the range of 200-300 nm), is without inter-columnar voids and dome shape column tops; also evident from the AFM image (figure 4b). However the microstructure of CA coatings can be greatly affected by the presence of droplets as the area surrounding these droplets is often under-dense and disturbed.

## C. Corrosion performance

Figure 5a shows the polarisation curves obtained for both the coatings. The $E_{corr}$ value (around - 330 mV) and the anodic corrosion currents of H+U coating were found to be near identical to that of the CA coating up to 150 mV. However H+U coating system exhibits a higher tendency to passivate (reduction in corrosion currents) in the range of 150 mV to 370

mV as compared to CA coating. Since Zirconium has a tendency to passivate around the potential range 150 to 370 mV and for the pH values employed in the experiments conducted,[20] any corrosion current contributions in these conditions will be highly influential by the substrate corrosion. Time elapsed substrate exposure through defects and its passivation will dominate the corrosion mechanisms in the above potential range (150 to 370 mV). Figure 5b shows the as deposited surface of the H+U coating where no droplet defects are visible whereas figure 5b shows the CA surface with droplet defects. As evident from the polarisation curves and figures 5b and 5c, defective microstructure surrounding the droplet defects in the CA coatings can be attributed for the rise in corrosion currents for CA coatings in these conditions.

### D. Stochiometry and Spectrophotometery Analysis

The H+U coatings appeared bright yellow with a small contribution from green. The values 78.42, 2.64 and 37.98 corresponding to L*, a* and b* respectively were measured by averaging results from 3 different spots. Similarly CA coatings appeared whiter than H+U coatings and had the L*, a* and b* co-ordinates as L* -89.23, a*= -1.78 and b*= 16.73. Electron Probe Micro Analysis (EPMA) confirmed the H+U coatings to be near stoichiometric with a N: Zr ratio of 1.2 whereas the CA coatings were found to be slightly sub-stoichiometric with a N: Zr ratio of 0.45.

## IV. Conclusions

1. Zirconium nitride (ZrN) PVD coatings were successfully deposited with the combined HIPIMS and UBM technology in an industrial sized Hauzer HTC-4 1000 PVD coater enabled with HIPIMS technology.

2. HIPIMS assisted UBM deposited coatings have clean and sharp substrate-coating interfaces with evidence of large area epitaxial growth of coating promoting high adhesion (in excess of 100 N) comparable to CA deposited coatings. The results show dense columnar grain microstructure (absence of inter-columnar voids), equally dense to

that of CA however without droplets and associated defects. This is a result of high ad-atom mobility resulting from intense low energy ion bombardment.

3. Superior microstructures of H+U coating resulted in mechanical properties comparable (high adhesion >100N, high hardness) or better than CA coatings (sliding wear coefficients ($K_c$) of 5.33 x $10^{-15}$ and 8.01 x $10^{-15}$ respectively).

4. Corrosion performance of the H+U coating is superior to that of the CA coatings as evident from the passivating behaviour of the coating-substrate system in the potential range (150 to 370 mV).

5. H+U technique can be a good alternative to CA where smooth, dense coatings are required and macro droplets cannot be tolerated.

## References


[1] Y. P. Purandare, A. P. Ehiasarian and P. Eh. Hovsepian, J. Vac. Sci. Technol. A 26, 288 (2008).

[2] P.E. Hovsepian, A.P. Ehiasarian, Y.P. Purandare, R. Braun, I.M. Ross, Plasma Process. Polymer 6 (S1), S118 (2009).

[3] J.A. Thornton, J. Vac. Sci. Technol. 11, 666 (1974).

[4] P.E. Hovsepian, D.B. Lewis, W.-. Münz, Surf. Coat. Tech. 133-134**,** 166 (2000).

[5] I. Petrov, P. Losbichler, D. Bergstrom, J.E. Greene, W.-. Münz, T. Hurkmans, T. Trinh, Thin Solid Films, 302, 179 (1997).

[6] K.A. Gruss, T. Zheleva, R.F. Davis, T.R. Watkins, Surf. Coat. Tech. 107, 115 (1998).

[7] A.P. Ehiasarian, P.E. Hovsepian, L. Hultman, U. Helmersson, Thin Solid Films 457, 270 (2004).

[8] P.C. Johnson and H. Randhawa, Surf. Coat. Tech. 33, 53 (1987).

[9] W.D. Sproul, Thin Solid Films 107, 141 (1983).

[10] S. Heinrich, S. Schirmer, D. Hirsch, J.W. Gerlach, D. Manova, W. Assmann, S. Mändl, Surf. Coat. Tech. 202, 2310 (2008).

[11] A.P. Ehiasarian, W.-. Münz, L. Hultman, U. Helmersson, I. Petrov, Surf. Coat. Tech. 163-164**,** 267 (2003).

[12] K. Sarakinos, J. Alami, S. Konstantinidis, Surf. Coat. Tech. 204**,** 1661 (2010).

[13] A. Anders, Vacuum 67 (3–4), 673 (2002).

[14] Y.P. Purandare, A.P. Ehiasarian, P.E. Hovsepian, J. Vac. Sci. Tech. A 29, 011004 (2011).

[15] A. P. Ehiasarian, J. G. Wen, I. Petrov, J. Appl. Phys. 101**,** 054301 (2007).

[16] D. Pilloud, A.S. Dehlinger, J.F. Pierson, A. Roman, L. Pichon, Surf. Coat. Tech. 174-175, 338 (2003).

[17] D.F. Arias, Y.C. Arango, A. Devia, Appl. Surf. Sci. 253, 1683 (2006).

[18] H. Jiménez, E. Restrepo, A. Devia, Surf. Coat. Tech. 201, 1594 (2006).

[19] Y.P. Purandare, A.P. Ehiasarian, P.E. Hovsepian, J. Vac. Sci. Technol. A 26**,** 288 (2008).

[20] Marcel Pourbaix, *Atlas of Electrochemical Equilibria in Aqueous Solutions* (NACE, Houston, TX 1966).

**Table 1** : Characterisation results.

| **Deposition technique** | **Thickness** | **Residual stress [GPa]** | **Nano hardness [GPa]** | **E(O&P) [GPa]** | **Scratch Test ($L_C$)** | **Sliding wear(Kc) [$m^3N^{-1}m^{-1}$]** |
|---|---|---|---|---|---|---|
| H+U | 2.5 ± 0.2 µm | - 4.12 ± 0.2 | 35 ± 3 | 410 ± 3 | > 100 N | $5.33 \times 10^{-15}$ |
| CA | 2.5 ± 0.2 µm | - 5.82 ± 0.3 | 37 ± 3.4 | 487± 2 | > 100 N | $8.01 \times 10^{-15}$ |

**Table 2:** Crystallite sizes and lattice strains of HIPIMS+UBM and Cathodic Arc ZrN coating calculated from the XRD peaks.

| | *H+U coating* | | *CA coating* | |
|---|---|---|---|---|
| **Orientation** | **Crystallite size [nm]** | **Lattice strain [%]** | **Crystallite size [nm]** | **Lattice strain [%]** |
| **111** | 9.1 | 1.654 | 18.0 | 0.981 |
| **200** | 9.5 | 1.376 | 23.6 | 0.693 |

## Figure Caption List

**Figure 1 (colour online):** XRD patterns obtained with a Bragg-Brentano technique for the substrate and ZrN coated specimens.

**Figure 2:** TEM bright-field image with selected area diffraction patterns of the HIPIMS+UBM coating.

**Figure 3**: TEM bright-field image with selected area diffraction patterns of the Cathodic Arc coating.

**Figure 4 (colour online):** AFM images of the as deposited (a) HIPIMS+UBM coating (b) Cathodic Arc coating.

**Figure 5 (colour online)**: (a) Polarisation curves for HIPIMS+UBM and Cathodic Arc coatings. SEM micrographs of the as deposited coating surface (b) HIPIMS+UBM coating (c) Cathodic Arc coating.

**Figure 1**

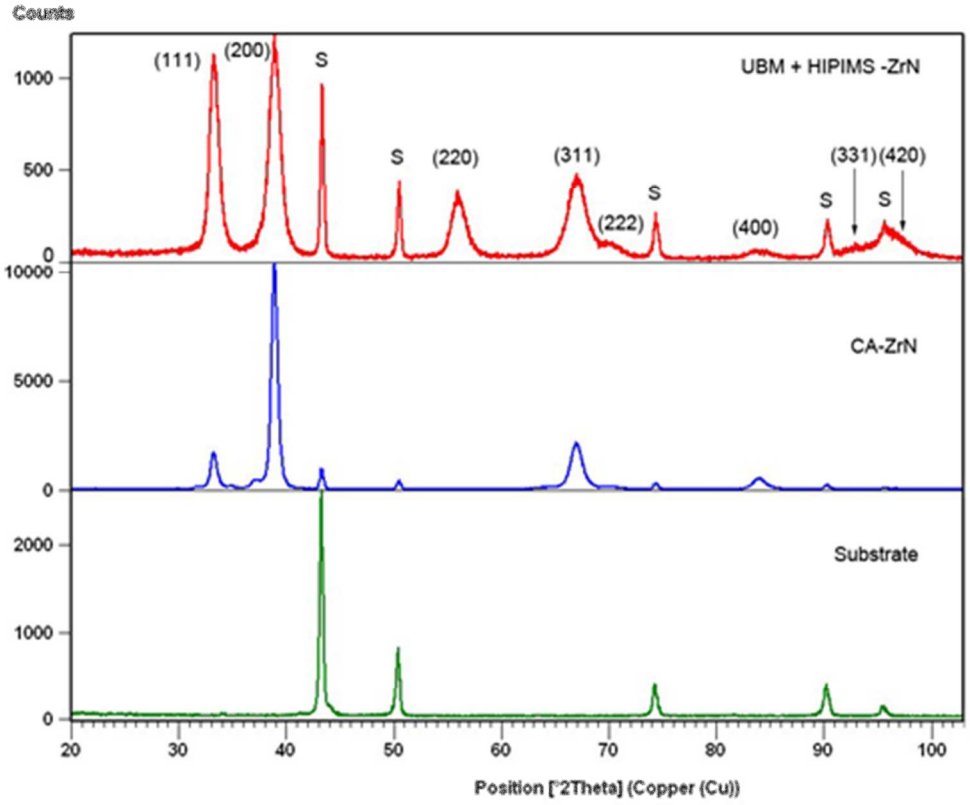
Counts
(111)
(200)
S
S
(220)
(311)
(222)
S
(400)
S
(331)
(420)
S
UBM + HIPIMS -ZrN
CA-ZrN
Substrate
1000
500
0
10000
5000
0
2000
1000
0
20
30
40
50
60
70
80
90
100
Position [°2Theta] (Copper (Cu))

**Figure 2**

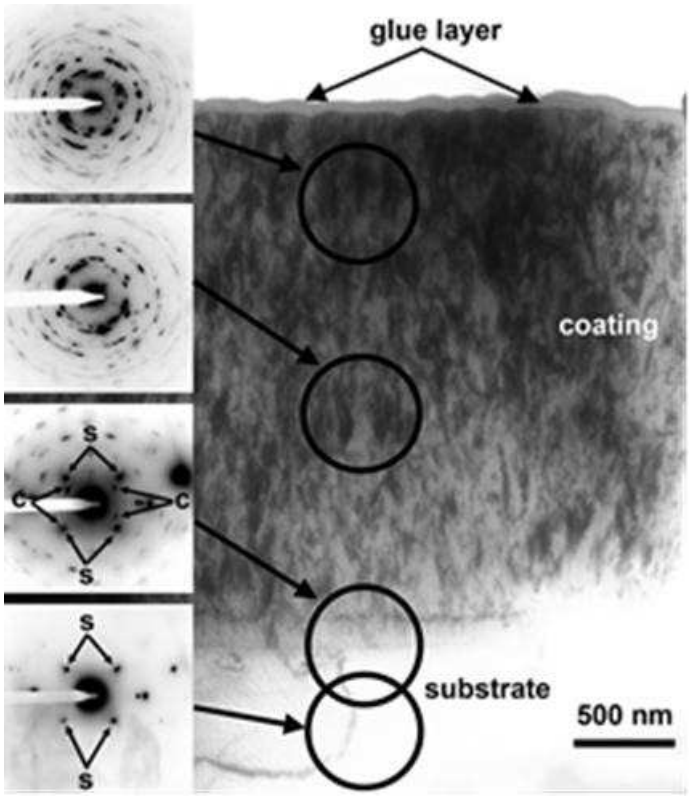

**Figure 3**

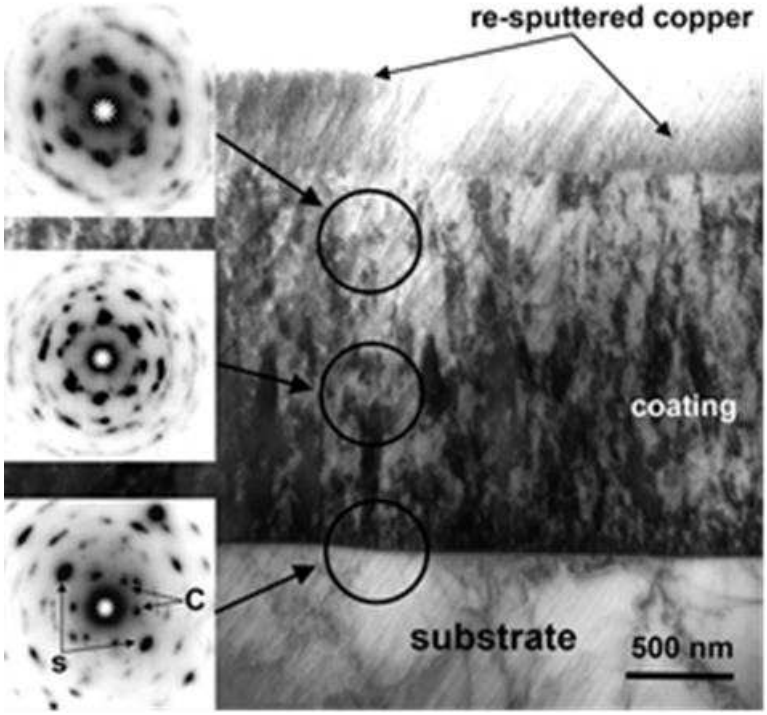

**Figure 4**

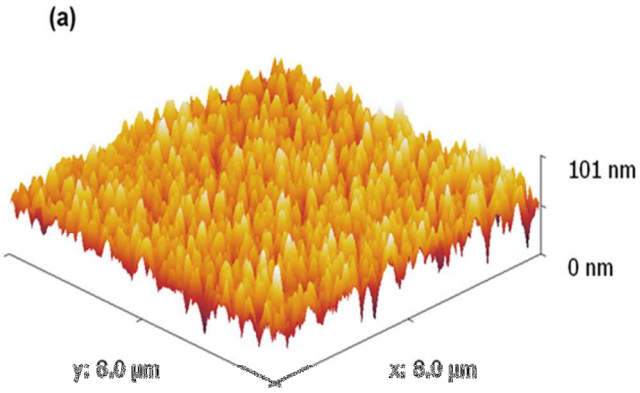


H/U coating surface

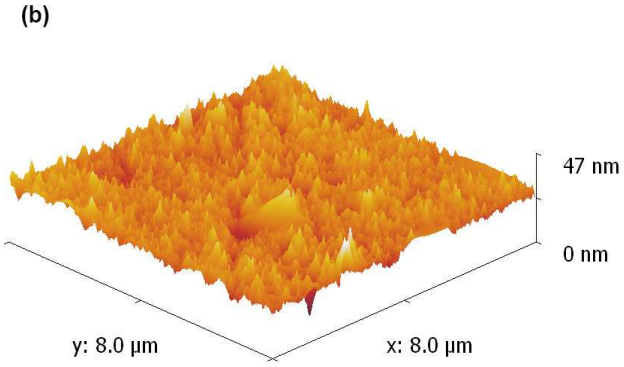


CA coating surface

**Figure 5**

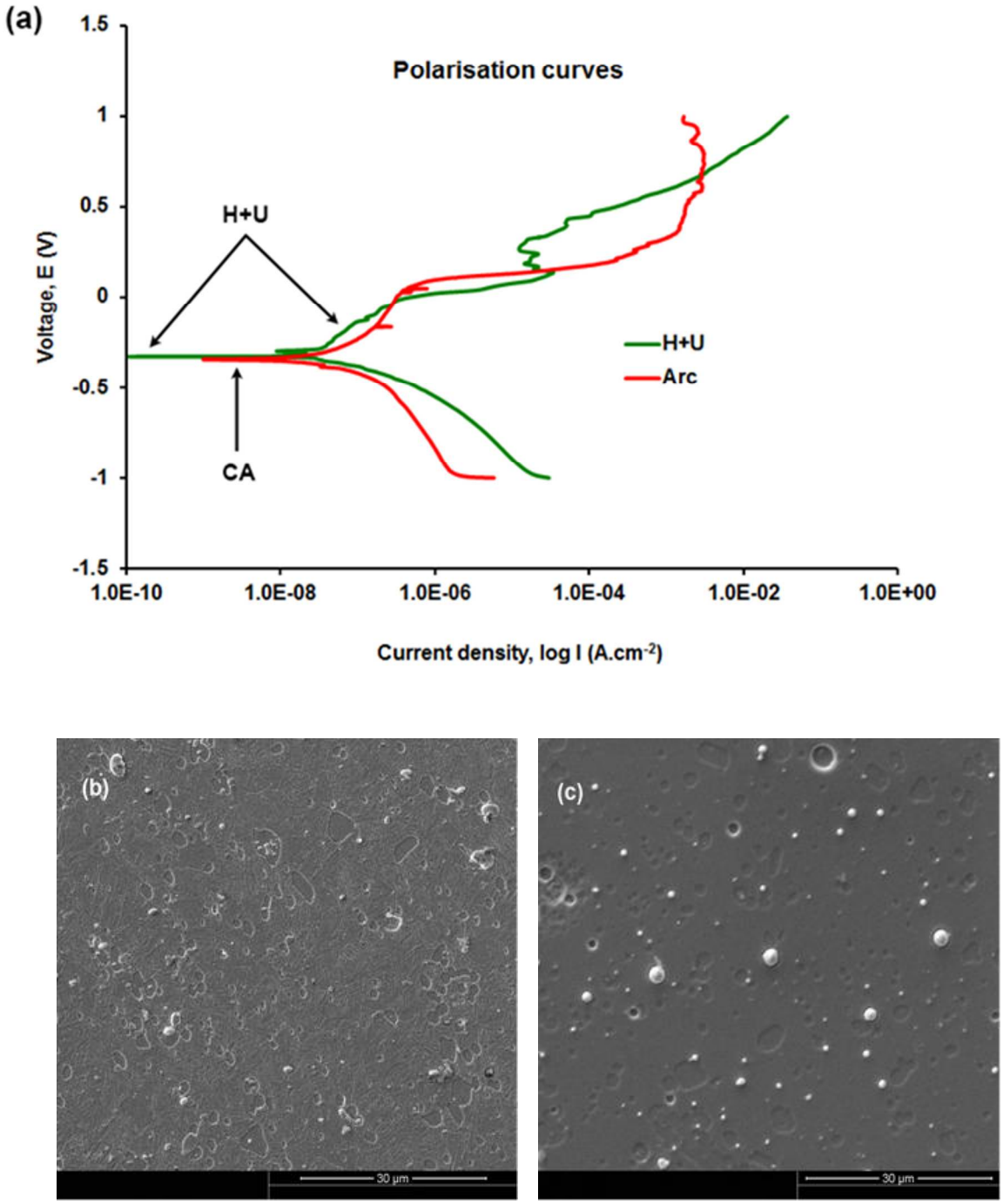
(a)
Polarisation curves
Voltage, E (V)
1.5
1
0.5
0
-0.5
-1
-1.5
H+U
CA
H+U
Arc
1.0E-10
1.0E-08
1.0E-06
1.0E-04
1.0E-02
1.0E+00
Current density, log I (A.cm-2)
(b)
30 µm
(c)
30 µm